RSC Publishing Faraday Discussions

FD 177: Phase Modulation Nanoscopy: a simple approach to enhanced optical resolution

Journal:	*Faraday Discussions*
Manuscript ID:	FD-ART-08-2014-000158.R1
Article Type:	Paper
Date Submitted by the Author:	04-Nov-2014
Complete List of Authors:	Pal, Robert; Durham University, Chemistry

Phase Modulation Nanoscopy: a simple approach to enhanced optical resolution

Robert Pal*

Department of Chemistry, Durham University, South Road, DH1 3LE Durham United Kingdom. Email: robert.pal@dur.ac.uk
DOI: 10.1039/b000000x [DO NOT ALTER/DELETE THIS TEXT]

A new modular super-resolution technique called Phase Modulation Nanoscopy (PhMoNa) has been developed in order to break the optical diffraction barrier in Confocal Laser Scanning Microscopy (LSCM). This technique is based on using spatially modulated illumination intensity, whilst harnessing the fluorophore's non-linear emission response. It allows experimental resolution in both lateral and axial domains to be improved by at least a factor of 2. The work is in its initial phase, but by using a custom built Electro Optical Modulator (EOM) in conjunction with functionalised Ln(III) complexes as probes, a sub-diffraction resolution of ~60 nm was achieved of selected cellular organelles in long term live cell imaging experiments.

Introduction

In the field of optical fluorescence microscopy, many researchers have dedicated their entire scientific carrier to develop better and improved cellular stains or associated microscopy techniques and equipment, pushing the boundaries of both signal detection and resolution. However, the intrinsic resolution of fluorescence microscopy is limited by diffraction, which determines the extension of the focused light emitted by a point source object, in other words the point spread function (PSF). In recent years, renewed have efforts emerged in optical microscopy and associated life sciences to break through the optical diffraction barrier and visualize even smaller parts of the 'living' cell in 'super-resolution'. Governed by Abbé's law (1873) the highest achievable theoretical spatial resolution (d) of a given experimental setup is dictated by the lowest applied excitation light (λ_{exc}) $d = \lambda_{exc}/2NA$ (NA: numerical aperture of objective).[1,2] Almost all commercially available cellular stains and subsequently the majority of 'off-the-shelf' microscopes are equipped with light sources possessing excitation wavelengths ≥405 nm through the visible and NIR promoting maximal achievable resolutions of ~200 nm.[3] However, much of the fundamental biology of the cell occurs below this threshold; hence breaking this limit will allow the wide multidisciplinary scientific community to look deeper in higher resolution.

As noted by Köhler in the beginning of the 20th century, one of the simplest experimental modification to improve lateral resolution is to illuminate samples using shorter wavelength ultra violet (UV) light.[4] This technique was fully exploited in the early days of microscopy and has always been associated with unwanted auto-fluorescence from endogenous chromophores and more importantly disruptive UV induced processes, such as DNA damage leading to high photo-toxicity.[5] Thus, the

approach of improved resolution, ever since the step-changing invention of Confocal Microscopy by Minsky in 1953,[6,7] has turned towards the development of new optical (hardware) and computer (software) based methodologies,[8,9] revolutionising the way in which we investigate nanostructures. The current key technologies are: SIM, where structured patterns are introduced into the illumination pathway ($d_{latheral}$ = 100-120 nm),[10–12] RESOLFT, which utilises quantum effects to spatially inhibit the applied stains fluorescence (e.g. STED which is currently the most sought after and applied commercially available technique, 20-100 nm).[13–15] These techniques dominate alongside near-field nano-scanning technique utilising a propagating evanescent wave NSOM (20-120 nm),[16,17] and the pointillistic localisation methods PALM/STORM (20-50 nm)[18,19] using photo-switchable fluorophores. Recent years seen many refined and evolved variants of the above mentioned techniques by improvements applied either or both to the illumination or detection process leading to improvement in both precision and resolution. But these new, still fundamentally diffraction limited techniques all have drawbacks too, such as limitation of suitable stains, disruptively high laser powers, slow/limited imaging speed, poor SNR due to loss of information and specialized expensive and bulky instrumentation. Taking the above into account, the obvious conclusion is to revisit the use of near-UV excitation with tailored bright and non-invasive molecular probes to investigate cellular organelles in finer detail. The primary future research aim renders itself to introduce a novel user friendly resolution enhancing method into any LSCM microscope harnessing the already superior resolution[20] of the confocal detection principle.

Methods and Results

The instrumental technique detailed herein, is currently still in the development phase and is predominantly used in conjunction with bright luminescent lanthanide probes recently developed in Durham.[21,22] In the future, it aims to be used with any currently existing LSCM microscope with high speed acquisition and improved resolution of ~60 nm (achievable lateral resolution when coupled to a suitable 355nm light source). The use of well-designed lanthanide complexes as probes for spectroscopy or microscopy can be advantageous due to their unique properties.[23,24] They exhibit long-lived emission (µs-ms), typically many orders of magnitude longer than that of background bio-auto-fluorescence (ns, similar lifetime as commercial organic cell stains), allowing for facile time-gated detection.[25] They have large *pseudo*-Stokes' shifts of hundreds of nanometers and possess well-defined, narrow peaks in the emission spectrum that can be exploited for more complex analysis.[26] Several examples exhibit dynamic responses to local conditions such as pH,[27–29] citrate[30] or bicarbonate[31], allowing the measurement of these species within particular organelles of mammalian[32] or plant cells.[33]

Fluorescence confocal microscopy is characterised by rather low SNR. However this can be boosted by pixel or line average scanning or multiple line or frame accumulation. This is an obvious trade off with acquisition speed as it prolongs scan intervals and subsequent, often disruptive specimen light exposure. However, with the new and higher sensitivity detectors, scan speed can be increased whilst excitation power can be minimised to trigger good SNR probe fluorescence

response, leading to exponentially lower levels of excitation exposure.

The experimental setup detailed herein is based on a novel combined structured illumination technique, where the region of support of the Optical Transfer Function (OTF) has been doubled leading to reciprocal sharpening of the Point Spread Function (PSF).[11] The approach uses a sequential frequency matched 3D oscillation of a carefully chosen optical grating (OG, paired with a corresponding first order filter) in the illumination beam path, inducing synchronized spatial periodicity (spatially modulated illumination intensity fluctuation, in other words, disruption in coherence) into the raster scanned (flying spot) excitation laser beam (*Figure 1. upper*).[34] Images recorded under such experimental conditions due to the frequency mixing of the sub-diffraction limited structure of the sample and the scanning patterned excitation cluster displays low frequency Moiré fringes. Simultaneously, this can easily be resolved and sub diffraction resolution images can be reconstructed in situ through automated synchronised image averaging.

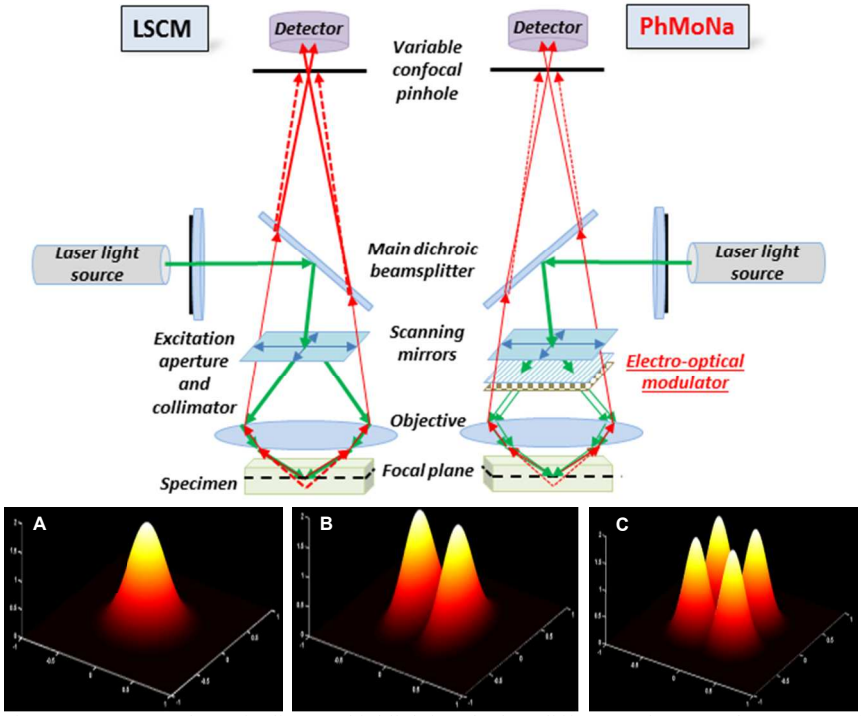

Figure 1. (upper) Schematic diagram highlighting the key differences between the LSCM and PhMoNa microscope hardware and light path. (lower) Theoretical evolution of the excitation beam profile: (A) standard CLSM, (B) 1D-EOM oscillation and (C) 2D-EOM oscillation PhMoNa at identical scan speeds (100 Hz) x and y in Airy units (AU, using $\lambda_{exc.}$ 355 nm and 1.4 NA). PSF calculations were based on the findings of Cremer and Heintzmann.[10]

In essence, Phase Modulation Nanoscopy (PhMoNa) operates by utilizing the optical grid pattern projected by the scanned first order diffracted excitation beam projected onto the back focal plane of the objective. This structured light modulation introduces high spatial frequencies in the illuminating light, whilst also acting as a

finite detection mask, leading to an advantageous shift of the observed finite objects spatial frequencies to generate improved experimental resolution.

Gaussian beam profile calculations (*Figure 1. lower*) revealed that this scan frequency matched synchoronised grid oscillation provides the best and hence fastest results, *e.g.* least number of averaged iteration is needed per scan to result in an evenly illuminated flat field of view (FOV), when the generated excitation pattern resembles a cluster of four identically symmetric beams (n = 4). Theoretically, subsequent n^2 splitting of the beam could improve the achievable resolution even further. However, it needs to be considered that to achieve the same unified beam height, in more simplistic terms excitation power delivery and subsequent fluorescent response, the spatial merge of neighbouring Gaussian beams (ρ, bleeding-in factor) would be substantial ($\rho^n = \sqrt{\pi} = 0.18$ when n = 4). This undesired spatial light saturation would lead to the recombination of the induced finite excitation pattern, consequently degrading the experimental resolution to the orders of a standard CLSM. Another advantageous consequence of forming such a structured excitation pattern is the inherent sharpening of the individual excitation PSFs. Preliminary results obtained, using our modified Leica SP5 II LSCM system, revealed that phase modulation induced transversal momentum disruption of the excitation laser beam can sharpen the experimental PSF by a factor of $[2\pi/\sqrt{(2\pi)}]*(1-\rho^n) = 2(.05)$ (n =4), eliminating spectral focal blur (*e.g.* pixel-cross-talk and saturation) by completely suppressing spatial frequencies outside the OTF, and subsequently improving lateral resolution at least two-fold.[11] It needs to be emphasized that in order to regain identical laser density, whilst recording identical levels of fluorescence probe response (*i.e.* similar even image brightness) a carefully synchronised individual frame or line Nyquist sampling rate of n^x=4 averaging (n=2, and as 2D diagonal EOM oscillation x=2) needed to be introduced to compensate for loss of fluorescence. This loss is attributed to offset selective masking of neighbouring pixels in the detection pathway with each line scan introduced by the synchronised EOM. This subsequently prolongs frame acquisition times four fold however, the overall Airy disk (AD) light exposure levels in 3D-Fourier space are maintained constant throughout, leading to an inherent two fold improvement in axial resolution and SNR. This simplistic optical modulation to the excitation path of a CLSM using a previously reported Europium(III)-9N3 complex[21] revealed, that improved lateral (~60 nm) and axial resolution (~200 nm both at 1.40NA) can be achieved (*Figure 2.*) using functionalised lanthanide complexes and a linearly polarised CW-NdYAG laser (3^{rd} harmonic at 355 nm).

The overall 8 fold reduction in experimental voxel size has been achieved, as the optical sectioning pinhole diameter, determining axial resolution, has been kept at 0.5 AU throughout. The value has been automatically calculated using the FWHM of the individual Gaussian beam generated in the scanning excitation cluster.[35,36] Further reduction of the confocal pinhole diameter could result in achieving a unified voxel of a^3 (a = 62 nm). However, due to reduction of the studied optical section thickness loss in fluorescence emission could only be compensated by increase in applied laser power that could lead to undesired photo-induced probe and cell damage resulting in shortened live cell experiments.

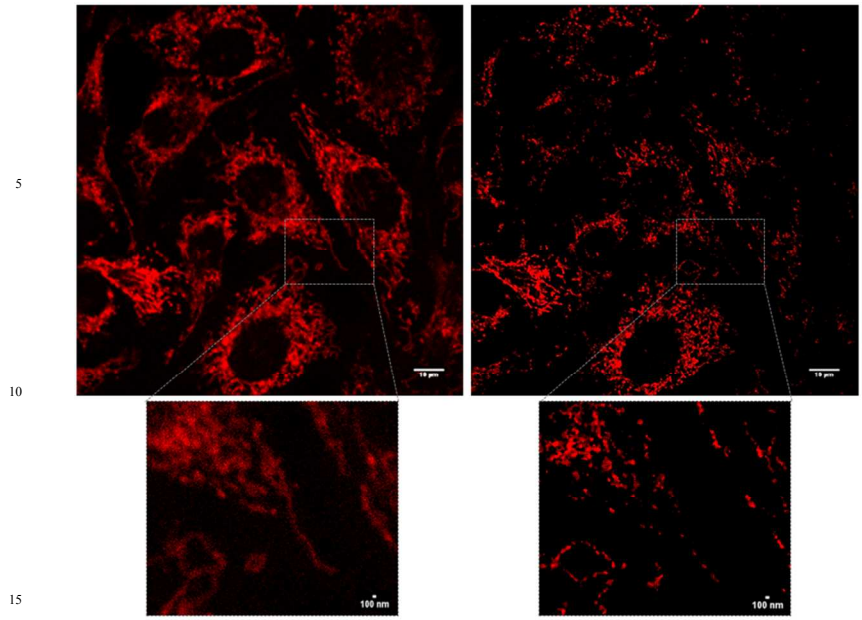

Figure 2. Comparison of CLSM (*top left) and* PhMoNa enhanced LSCM (*top right*) live cell images of the same FOV using a Eu(III)dye[21] ($C_{loading}$= 10 µM, λ_{ex} = 355 nm) revealing enhanced 62 nm lateral resolution (100 Hz, 2 line accumulation and 4 frame averaging sequence, 2048 x 2048 pixel scan on the Leica SP2 II,) of the mitochondrial network of NIH 3T3 cells. Total time of scan: LSCM 40 sec, PhMoNa 160 sec. Voxel size: CLSM 126 x 126 x 390 nm, PhMoNa: 63 x 63 1x 195 nm; scalebars are 10 µm. (*Bottom*) digital magnification of highlighted sections as indicated for LSCM (*left*) and PhMoNa (*right*) respectively; scalebars are 100 nm.

Functionalised lanthanide(III) complexes possess unique bio- and spectrophysical properties, such as long luminescence lifetimes (orders of ms), large *pseudo*-Stokes'-shift (Eu(III): 200 nm) and broad range (150 nm) yet finite structured emission profiles.[26,37–39] Due to the high brightness and cellular accumulation of such probes, we minimize the exposure to UV excitation below non photo-damaging level during live cell imaging experiments. Subsequent modular instrumental development also facilitated time-resolved imaging, spectral and lifetime profiling of the internalised dyes and probes.[32,40] The drawback, in this case, is that lanthanide probes possess low photo emission rates. However, this has proven to be an advantage in this early developmental stage, by allowing slow scan speeds to be used (10 Hz, 100 ms/pixel laser dwell time) while precise synchronisation of the structured illumination process was established. Once this sequence has been experimentally incorporated and validated, as a result of probe brightness, the scan speed and subsequent excitation patterning could be increased (up to 400Hz has been used), resulting in faster overall image acquisition times. It is also important to emphasize that by using luminescent lanthanide complexes, it is possible to achieve time-resolved (TR-)PhMoNa. Such a technique will not only eliminate the spatial focal blur contribution of UV induced short lived (ns) auto-fluorescence from endogenous chromophores and subsequently improve SNR, but also will drastically reduce photo-exposure of the cell due to pulsed excitation. These experimental aspects will also further prolong the observed cells natural homeostatic state and

minimise long term probe photo-bleaching whilst retaining optimal scanning speed. Another advantage to be explored in the future could be to facilitate biologically favourable multi-photon excitation (range 730-770 nm) with these bright lanthanide stains that also possess improved two photon cross-section.[32] This is an important point to make that as with the application of tuneable (380–2200 nm broad spectral range) White Laser Light (WLL) sources the need of expensive quartz optical elements ($\lambda_{exc.}$<355 nm) in the illumination path will be eliminated. Most importantly WLL-PhMoNa and its 8 fold overall experimental resolution improvement can be used with any commercially available cellular stain, at any given excitation wavelength on existing confocal microscopes, making it an attractive and affordable live-cell imaging technique to be used by the broad microscopy community.

Owing to its simplistic modular approach, PhMoNa can theoretically also be readily adapted to any preferred wavelength of excitation to achieve synchronised illumination-emission reduction, with a subsequent confocal voxel size reduction of a factor of 2^3 = 8 ($d_{lateral}$~$\lambda_{exc.}$/4). Thus, its versatility can be extended to any commercially available polarised laser excitation source. Since our test Leica SP5 II CLSM framework is equipped with 8 different laser lines (ranging from 355 – 633) attention has focused onto utilising our custom EOM to structure a more widely used laser line. Using the commercially available MitoTracker Green probe alongside the Eu(III) dye the EOM device has been incorporated into the optical path by placing it below the microscope objective. In this manner, both 355 and 488 nm identically oriented polarised laser lines were used simultaneously in a frame by frame recording sequence. Superior resolution images were captured, maintaining both scan speed and light exposure adequately in each channel (*Figure 3*.).

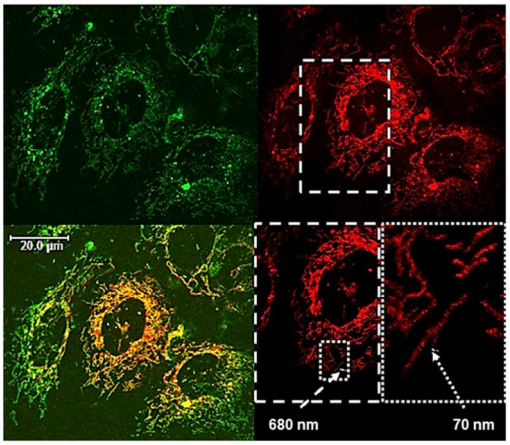

Figure 3. PhMoNa enhanced live-cell LSCM images of the Eu(III)dye[21] used (*Figure 2*.) above (*red*) ($C_{loading}$ =1 µM, 40 sec image acquisition, λ_{ex} = 355 nm) co-stained with MitoTracker Green (*green*) ($C_{loading}$ =200 nM, 40 sec image acquisition, λ_{ex} = 488 nm) revealing enhanced 62 nm (*red channel*) and 87 nm (*green channel*) lateral resolution respectively (400Hz, 2 pixel by pixel accumulation and 4 line-averaging sequence, smallest detectable individual pixel size using a 2048x2048 scan on the Leica SP2 II) of the mitochondrial network of NIH 3T3 cells. (*orange*) RGB merge to confirm co-localisation, (*bottom right*) digital magnification sequence (with respective scalebar values) to reveal 2-fold improved experimental latheral resolution.

One of the most important user friendly aspects to be considered with the above detailed experimental modification is in fact an inherent feature of the donor LSCM setup. In detail, due to the software determined line averaging sequence combined with the synchronised frequency matched nature of excitation cluster generation (i.e. spatially structured illuminating periodicity) during raster scanning, renders this technique free from any unnecessary time consuming post image processing deconvolution algorithm.

Conclusion and Future work

The primary aim was set to develop a low-cost super-resolution microscope creating a major a formidable advance over conventional LSCM. Initially the setup was tested with functionalised Ln(III) complexes, synthesized parallel to instrumental development in Durham. By employing a custom built Electro Optical Modulator (EOM) spatio-temporal evolution of a sinusoidal phase modulated laser beam has been carried out. The resulted modular attachment can be used in situ, as part of an existing LSCM instrument. The modified system has allowed even more detailed information of cellular substructures to be extracted at favourable high scanning speeds. Overall, identical laser power has been employed during PhMoNa recordings as were used with the standard LSCM images used for comparison. The only experimental difference was prolonging the scan time by a factor of four (up to 400 Hz scan speed), but strictly not the excitation exposure time (*i.e.* overall dwell time per pixel). It is extremely important to emphasize that this form of excitation PSF sharpening technique is only in its early phase and introducing an optical element oscillating at high frequencies into any optical path can lead to unwelcomed vibration which can impair resolution. This was considered as being the major drawbacks of this technique, the other being the introduced four times increase in overall image acquisition. Hence, several novel approach using cleverly constructed new generation of EOMs are being currently developed to obviate this. Our aim still remains the modular attachment approach and not introducing a special cavity modulated laser to the setup to generate such finite excitation patterns. Once further developed, with a suitable EOM device to fulfil all our critical design criteria, PhMoNa may be employed as a cost effective ‘add-on’ resolution enhancing module to all LSCM.

In the future PhMoNa and its 8 fold overall experimental resolution improvement could be used with any commercially available or novel emerging (including both transition-metal and lanthanide complexes) cellular stain, at any given excitation wavelength on any existing confocal microscopes, making it an attractive and affordable live-cell imaging technique, to be used by the broad microscopy community Thus, saturation eliminated high spatial resolution 3D reconstructions can be created maintaining fast scan speed, low laser power and exposure time inherently minimising photo-bleaching. Another important advantage to emphasize is that PhMoNa promises to be one of the few applicable experimental nanoscopy techniques that can be used safely for live-cell imaging, eliminating the need for tedious after image processing algorithms.

Acknowledgements

I would like to express my sincere gratitude to Professor David Parker for his expert help and guidance on lanthanide(III) complexes, Prof. Andrew Beeby for his time and devotion on optical detection optimisation, Mr. Kelvin Appleby (Electrical Workshop) for all his valuable expertise and work on electric components, and EPSRC, ERC and Royal Society URF for the funding.

References

1. E. Abbe, *Arch. Für Mikrosk. Anat.*, 1873, **9**, 413–418.
2. Rayleigh, *Philos. Mag. Ser. 5*, 1896, **42**, 167–195.
3. D. Spector and R. D. Goldman, *Basic Methods in Microscopy Protocols and Concepts from Cells: A Laboratory Manual*, Book News Inc, 2006.
4. A. Köhler and W. Loos, *Naturwissenschaften*, 1941, **29**, 49–61.
5. J. C. F. Wong and A. V. Parisi, 2nd Internet Conference on Photochemistry and Photobiology: Protection Against the Hazards of UVR, 1999.
6. M. Minsky, *Scanning*, 1988, **10**, 128–138.
7. C. Cremer and T. Cremer, *Microsc. Acta*, 1974, 31–44.
8. L. Schermelleh, R. Heintzmann and H. Leonhardt, *J. Cell Biol.*, 2010, **190**, 165–175.
9. S. Habuchi, *Front. Bioeng. Biotechnol.*, 2014, **2**.
10. R. Heintzmann and C. G. Cremer, 1999, vol. 3568, pp. 185–196.
11. M. G. L. Gustafsson, *J. Microsc.*, 2000, **198**, 82–87.
12. R. Heintzmann, *Micron*, 2003, **34**, 283 – 291.
13. S. W. Hell and J. Wichmann, *Opt Lett*, 1994, **19**, 780–782.
14. K. Willig, S. Rizzoli, V. Westphal, R. Jahn and S. Hell, *Nature*, 2006, **440**, 935–9.
15. T. A. Klar, S. Jakobs, M. Dyba, A. Egner and S. W. Hell, *Proc. Natl. Acad. Sci.*, 2000, **97**, 8206–8210.
16. E. Betzig and J. K. Trautman, *Science*, 1992, **257**, 189–195.
17. F. de Lange, A. Cambi, R. Huijbens, B. de Bakker, W. Rensen, M. Garcia-Parajo, N. van Hulst and C. G. Figdor, *J. Cell Sci.*, 2001, **114**, 4153–4160.
18. K. Lidke, B. Rieger, T. Jovin and R. Heintzmann, *Opt. Express*, 2005, **13**, 7052–7062.
19. S. T. Hess, T. P. K. Girirajan and M. D. Mason, *Biophys. J.*, 2006, **91**, 4258 – 4272.
20. O. Haeberlé and B. Simon, *Opt. Commun.*, 2009, **282**, 3657 – 3664.
21. S. J. Butler, L. Lamarque, R. Pal and D. Parker, *Chem Sci*, 2014, **5**, 1750–1756.
22. S. J. Butler, M. Delbianco, L. Lamarque, B. K. McMahon, E. R. Neil, J. W. Walton, R. Pal, D. Parker and J. M. Zwier, *Dalton Trans Perspect.*, 2014.
23. S. J. Butler and D. Parker, *Chem Soc Rev*, 2013, **42**, 1652–1666.
24. S. V. Eliseeva and J.-C. G. Bunzli, *Chem Soc Rev*, 2010, **39**, 189–227.
25. D. Parker and J. A. G. Williams, *J Chem Soc Dalton Trans*, 1996, 3613–3628.
26. C. P. Montgomery, B. S. Murray, E. J. New, R. Pal and D. Parker, *Acc. Chem. Res.*, 2009, **42**, 925–937.
27. B. K. McMahon, R. Pal and D. Parker, *Chem Commun*, 2013, **49**, 5363–5365.
28. R. Pal and D. Parker, *Org Biomol Chem*, 2008, **6**, 1020–1033.
29. D. G. Smith, B. K. McMahon, R. Pal and D. Parker, *Chem Commun*, 2012, **48**, 8520–8522.
30. R. Pal, D. Parker and L. C. Costello, *Org Biomol Chem*, 2009, **7**, 1525–1528.
31. D. G. Smith, G. Law, B. S. Murray, R. Pal, D. Parker and K.-L. Wong, *Chem Commun*, 2011, **47**, 7347–7349.
32. S. J. Butler, B. K. McMahon, R. Pal, D. Parker and J. W. Walton, *Chem. – Eur. J.*, 2013, **19**, 9511–9517.
33. A. Palmer, S. H. Ford, S. J. Butler, T. J. Hawkins, P. J. Hussey, P. Robert, J. W. Walton and D. Parker, *RSC Adv.*, 2014, **4**, 9356.
34. R. Heintzmann, T. M. Jovin and C. Cremer, *J Opt Soc Am A*, 2002, **19**, 1599–1609.
35. T. Wilson, *Confocal Microscopy*, London UK, 1990.
36. C. J. R. Sheppard, in *Scanning optical microscopy. In: Barer R and Cosslett VE (eds), Advances in Optical and Electron Microscopy 10*, Academic press, London UK, 1987.
37. J. W. Walton, A. Bourdolle, S. J. Butler, M. Soulie, M. Delbianco, B. K. McMahon, R. Pal, H. Puschmann, J. M. Zwier, L. Lamarque, O. Maury, C. Andraud and D. Parker, *Chem Commun*, 2013, **49**, 1600–1602.

38. E. J. New, D. Parker, D. G. Smith and J. W. Walton, *Curr. Opin. Chem. Biol.*, 2010, **14**, 238 – 246.
39. M. C. Heffern, L. M. Matosziuk and T. J. Meade, *Chem. Rev.*, 2014, **114**, 4496–4539.
40. R. Pal and A. Beeby, *Methods Appl. Fluoresc.*, 2014, **2**, 037001.